Food Chemistry 469 (2025) 142581

Contents lists available at ScienceDirect

Food Chemistry

journal homepage: www.elsevier.com/locate/foodchem

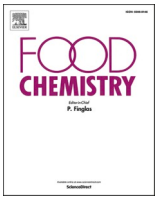

Effect of 4-methylbenzoquinone concentration on its covalent conjugates with β-lactoglobulin: Structural and functional properties

Jinshun Ye, Xiaotong Li, Zhenzhao Weng, Yuting Li *, Xiaozhen Liu, Xiangying Yu, Fengyuan Liu, Jingkun Yan, Lin Li

Engineering Research Center of Health Food Design & Nutrition Regulation, Dongguan Key Laboratory of Typical Food Precision Design, China National Light Industry Key Laboratory of Healthy Food Development and Nutrition Regulation, School of Life and Health Technology, Dongguan University of Technology, Dongguan 523808, China

ARTICLE INFO

Keywords:
4-Methylbenzoquinone
β-Lactoglobulin
Covalent interaction
Antioxidant activity
Emulsifying properties

ABSTRACT

This study examined the effect of quinone concentration on covalent interaction between β-lactoglobulin (β-Lg) and 4-methylbenzoquinone (4MBQ). β-Lg-4MBQ-0.2, β-Lg-4MBQ-0.4, and β-Lg-4MBQ-0.8 were prepared at 1:2, 1:1, and 2:1 M ratio of 4MBQ to β-Lg thiols, respectively. β-Lg-4MBQ-0.8 had the highest polyphenol content (19.04 ± 0.17 mg/g) and the lowest free sulfhydryl (17.12 ± 0.18 μmol/g) and amino group (181.28 ± 5.37 μmol/g) contents. Compared to β-Lg, β-Lg-4MBQ conjugates showed reduced α-helix (0.82–1.26 %) and increased β-sheet (1.17–1.50 %) content. β-Lg-4MBQ-0.8 and β-Lg-4MBQ-0.4 exhibited higher surface hydrophobicity and emulsifying properties than β-Lg-4MBQ-0.2 and β-Lg. Antioxidant activity (DPPH and ABTS scavenging) followed: β-Lg-4MBQ-0.8 (46.75 ± 0.17 % and 50.97 ± 0.51 %) > β-Lg-4MBQ-0.4 (39.50 ± 0.27 % and 46.63 ± 0.59 %) > β-Lg-4MBQ-0.2 (33.35 ± 0.71 % and 43.00 ± 0.39 %) > β-Lg (31.50 ± 0.56 % and 36.25 ± 0.90 %). β-Carotene emulsions stabilized by β-Lg-4MBQ-0.4 exhibited the highest stability. These findings provide insights into developing antioxidant emulsifiers.

1. Introduction

β-Lactoglobulin (β-Lg), the principal constituent of bovine whey protein, is extensively utilized as an emulsifier in food processing due to its superior emulsifying properties. Oil-in-water emulsions stabilized by β-Lg can be employed for the encapsulation of a range of bioactive compounds, including β-carotene (Qian, Decker, Xiao, & McClements, 2012) and coenzyme Q10 (Lee, Choi, Ha, & Lee, 2013). Components that promote lipid oxidation, such as transition metal ions, enzymes, and photosensitizers, are typically found in the aqueous phase of food emulsions. These components, or the free radicals induced by them, diffuse to the oil-water interface, initially causing oxidation of interfacial lipids, which then propagates to the interior of the oil droplets (McClements & Decker, 2018). Therefore, enhancing the antioxidant properties of the oil-water interface is essential for improving the overall stability of emulsions, which can be achieved by modifying proteins to boost their antioxidant capabilities.

Proteins can engage in covalent interactions with polyphenols, resulting in the formation of conjugates that exhibit enhanced antioxidant properties. Additionally, these conjugates often demonstrate superior emulsifying characteristics compared to the native proteins. The conjugates formed by the covalent interactions of β-Lg with chlorogenic acid, epigallocatechin-3-gallate (EGCG), and gallic acid exhibited significantly enhanced antioxidant properties, emulsification activity index (EAI), and emulsification stability index (ESI) compared to β-Lg alone (Man et al., 2024). Similarly, the covalent conjugation of rosmarinic acid with β-Lg was found to significantly enhance the interfacial wettability, EAI, ESI and antioxidant capacity of β-Lg (Y. Wang et al., 2024). Quinone-mediated covalent bonding is one of the primary mechanisms for forming polyphenol-protein conjugates (Li et al., 2024). The synthesis of polyphenol-protein covalent adducts via quinone-mediated reactions generally entails the combination of polyphenolic compounds with proteins, subsequently exposed to oxidizing conditions such as alkaline pH (Y. Wang et al., 2024), transition metal ions (Yin, Hedegaard, Skibsted, & Andersen, 2014), or oxidases (Ali, Keppler, Coenye, & Schwarz, 2018). Initially, polyphenols undergo oxidation to form corresponding quinones, which subsequently react with nucleophilic groups on the protein side chains, resulting in the formation of

* Corresponding authors at: School of Life and Health Technology, Dongguan University of Technology, Dongguan 523808, China.
E-mail address: liyt@dgut.edu.cn (Y. Li).

https://doi.org/10.1016/j.foodchem.2024.142581
Received 7 August 2024; Received in revised form 4 December 2024; Accepted 18 December 2024
Available online 19 December 2024

covalent adducts. However, the aforementioned methods do not allow for the measurement or control of quinone concentrations within the reaction system. Since the concentration of quinones affects the involvement of nucleophilic residues on protein side chains (Li et al., 2024), it may consequently influence the structure and functional properties of the covalent conjugates. Therefore, controlling quinone concentrations is essential for optimizing the functional properties of these conjugates.

4-Methylcatechol (4MC) is often employed as a model compound in *o*-phenol studies (Li et al., 2024). Oxidation of 4MC via bulk electrolysis (Li, Jongberg, Andersen, Davies, & Lund, 2016) or chemical methods (Waqar et al., 2022) can achieve the synthesis of 4-methylbenzoquinone (4MBQ) with yields exceeding 80 %. This is one of the rare *o*-quinone that can be successfully synthesized (Li et al., 2024). Previously studies have synthesized β-Lg-4MBQ covalent conjugates at a molar ratio of 1:1 (4MBQ to β-Lg) and investigated both their covalent binding sites (J. Liu et al., 2024) and digestibility (Waqar et al., 2022). As the concentration of 4MBQ increases in the reaction system, an increased number of lysine residues in β-Lg are involved in the covalent interaction (Li et al., 2024). The effects of 4MBQ reaction with β-Lg on the protein's structural and functional properties remain unclear, particularly with regard to how quinone content may influence these properties in polyphenol-protein conjugates. It is hypothesized that variations in quinone content could exert a significant impact on both the structural and functional characteristics of the conjugates.

Free thiol groups on proteins are recognized as the primary sites for the reaction between proteins and quinones (Li et al., 2024; J. Liu et al., 2024). In this study, the influence of 4MBQ concentration on the structural and functional properties of β-Lg-4MBQ covalent conjugates was investigated at quinone to β-Lg free thiol group molar ratios of 2:1, 1:1, and 1:2. These covalent conjugates were then employed to stabilize β-carotene emulsions. The stability of the β-carotene emulsions, stabilized by the β-Lg-4MBQ covalent conjugates, was subsequently evaluated during storage or under thermal treatment and light exposure.

2. Materials and methods

2.1. Chemicals and reagents

4-Methylcatechol (4MC, ≥96 %), β-carotene (≥96 %) were purchased from Aladdin (Shanghai, China). Soybean oil was supplied by Jinli-Oils & Fats Co., Ltd. (Suzhou, China). β-Lactoglobulin (β-Lg, ≥ 90 %) and 1-anilinonaphthalene-8-sulfonic acid (ANS, ≥ 97 %) were purchased from the Sigma-Aldrich (St. Louis, MO, USA). All other chemicals and reagents were of analytical grade.

2.2. Preparation of β-Lg-4MBQ covalent conjugates

4MBQ was prepared by bulk electrolysis of 2 mmol/L 4MC in a 0.2 mol/L NaH_2PO_4 solution as described in our previous study (Li et al., 2016). The yield of 4MBQ was approximately 83 %. β-Lg was dissolved in a 0.2 mol/L phosphate buffer at pH 7.0 to achieve a final concentration of 9 mg/mL. Subsequently, 4MBQ was introduced to this β-Lg solution to obtain mass ratios of 0.2 %, 0.4 % and 0.8 % (4MBQ/β-Lg, *w/w*, %), corresponding to molar ratios of 4MBQ to free thiols in β-Lg of 1:2, 1:1, and 2:1, respectively. 4MBQ-β-Lg covalent conjugates were then prepared according to the method outlined in our previous study (Li et al., 2024). β-Lg that reacted with 0.2 %, 0.4 % and 0.8 % 4MBQ were labeled as β-Lg-4MBQ-0.2, β-Lg-4MBQ-0.4 and β-Lg-4MBQ-0.8, respectively.

2.3. Characterization of β-Lg-4MBQ covalent conjugates

2.3.1. Total polyphenol content

The total polyphenol content of the β-Lg-4MBQ conjugates was determined using a modified Folin-Ciocalteu method (Y. Zhang et al., 2023). Initially, 0.5 mL of the β-Lg-4MBQ conjugate solution was thoroughly blended with 2.5 mL of 0.2 N Folin-Ciocalteu reagent and incubated at room temperature in the dark for 5 min. Next, 4 mL of 7.5 % (*w/v*) Na_2CO_3 solution was added. The solution was reacted in the dark at 25 °C for 2 h and then measured at 760 nm. The total polyphenol content was quantified using a 4MC standard curve and expressed in milligrams of polyphenols per gram of the sample (mg/g).

2.3.2. Free sulfhydryl and amino groups content

The free sulfhydryl group contents were analyzed by reacting with 5,5′-dithiobis (2-nitrobenzoic acid) (DTNB), following the method detailed in our previous study (Li et al., 2016).

The amino group contents were quantified as previously outlined (K. Dai et al., 2023). β-Lg and β-Lg-4MBQ conjugates were dissolved in phosphate buffer (pH 7.0, 10 mmol/L) at a concentration of 6.0 mg/mL. A 200 μL aliquot of the above solution was mixed with 4 mL of OPA reagent, incubated at 35 °C for 5 min, and the absorbance was subsequently measured at 340 nm. Amino group contents were determined using a glycine standard curve.

2.3.3. LC-MS/MS analysis of β-Lg-4MBQ covalent conjugates

β-Lg-4MBQ-2 underwent enzymatic hydrolysis, desalting, lyophilization and redissolution, followed by analysis using LC-MS/MS (Easy nLC-Q Exactive, Thermo Fisher Scientific, USA) described in our previous study (Li et al., 2024).

2.3.4. Ultraviolet-visible (UV–vis) and fluorescence spectroscopy

β-Lg and β-Lg-4MBQ conjugates were dissolved into phosphate buffer (10 mmol/L, pH 7.0) at a concentration of 0.5 mg/mL. UV–Vis spectra were subsequently obtained from 250 nm to 500 nm using an evolution 220 UV–Vis spectrophotometer (Thermo Fisher Scientific, USA) at 25 °C.

The endogenous fluorescence spectra of 0.2 mg/mL β-Lg and β-Lg-4MBQ conjugates in 10 mmol/L phosphate buffer (pH 7.0) were obtained using a F7100 fluorescence spectrometer (Hitachi, Japan). The operating parameters were as follows: emission wavelength of 300–500 nm, excitation wavelength of 280 nm, excitation slit of 5 nm and emission slit of 2.5 nm.

2.3.5. ATR-FTIR spectroscopy

The FTIR spectra of β-Lg and β-Lg-4MBQ conjugates were recorded using attenuated total reflection Fourier-transform infrared (ATR-FTIR) spectroscopy (Nicolet iS50, Thermo Fisher Scientific, USA) (Ding et al., 2024), with 32 scans at a resolution of 4 cm^{-1}.

2.3.6. Circular dichroism (CD) spectroscopy

β-Lg and β-Lg-4MBQ conjugate solutions were prepared in a phosphate buffer (10 mmol/L, pH 7.0) to a final concentration of 0.3 mg/mL. The CD of these solutions was measured using a Chirascan V100 circular dichroism spectrometer (Applied Photophysics, UK) over a wavelength range from 180 to 260 nm with a 0.5 mm path length. The content of α-helix, β-sheet, β-turn and random coil in the samples was calculated using CDNN software.

2.3.7. Particle size, ζ-potential measurements

β-Lg and β-Lg-4MBQ conjugate solutions were prepared as mentioned in 2.3.4. The particle size and ζ-potential of β-Lg or β-Lg-4MBQ conjugate were measured by Eclipse DualTec system (WYATT, USA) and a Zetasizer Nano-ZS90 analyzer (Malvern Panalytical, UK), respectively.

2.3.8. Colorimetric analysis

The color parameters of β-Lg and β-Lg-4MBQ conjugates were analyzed by a Konica Minolta CM-5 colorimeter. Three color coordinates were measured: L* representing lightness, a* indicating the green-to-red spectrum, and b* representing the blue-to-yellow spectrum. To

determine the color difference between β-LG and the β-LG-4MBQ conjugate, the following equation was employed:

$$\Delta E = \sqrt{\left(L_2^* - L_1^*\right)^2 + \left(a_2^* - a_1^*\right)^2 + \left(b_2^* - b_1^*\right)^2} \quad (1)$$

Here, L_1^*, a_1^*, and b_1^* represent the color metrics for β-Lg, whereasL_2^*, a_2^*, and b_2^* correspond to those of the β-Lg-4MBQ conjugate.

2.3.9. Surface hydrophobicity (H_0)

β-Lg and β-Lg-4MBQ conjugates were dissolved in 10 mmol/L phosphate buffer (pH 7.0) at concentrations ranging from 0.05 to 0.50 mg/mL. A 5 mL aliquot of the above solution was mixed with 20 μL of ANS (8 mmol/L), incubated in the dark for 5 mins, and analyzed using a fluorescence spectrophotometer following the method described by Man et al. (2024).

2.4. Antioxidant activity

The DPPH radical scavenging activity and ABTS radical scavenging activity of β-Lg and β-Lg-4MBQ conjugates were examined using methods reported in a previous study (Jing et al., 2020).

$$\text{DPPH}^{\bullet}\text{scavenging rate}\ (\%) = \left(1 - \frac{A_2 - A_1}{A_0}\right) \times 100 \quad (2)$$

$$\text{ABTS}^{\bullet+}\text{scavenging rate}\ (\%) = \left(1 - \frac{A}{A_0}\right) \times 100 \quad (3)$$

A_0 represents the absorbance of a standard prepared under the same conditions, but without the sample. A, A_1, and A_2 represent the absorbances of β-Lg and β-Lg-4MBQ conjugates, where A_1 is measured in the absence of DPPH solution.

2.5. Emulsifying properties

The EAI and ESI of β-Lg and β-Lg-4MBQ conjugates were assessed using methods described in a previous study, with slight modifications (Chen, Wang, Feng, Jiang, & Miao, 2019; Fan et al., 2019). A volume of 4 mL of β-Lg or β-Lg-4MBQ conjugate solutions (1 mg/mL) was blended with 1 mL of soybean oil using a T 10 basic high-speed homogenizer (IKA, Germany) at 10,000 rpm for 2 min to obtain an emulsion. Subsequently, 300 μL of the resulting emulsion was extracted from the bottom of the container, and 4.2 mL of 0.1 % (*w/v*) sodium dodecyl sulfate (SDS) was added to this aliquot. The absorbance of this diluted emulsion was measured at 500 nm initially and again at 15 mins. The EAI and ESI were calculated using the following equations:

$$\text{EAI}\left(m^2/g\right) = \frac{2 \times 2.303 \times A_0 \times N}{C \times \varphi \times 10000} \quad (4)$$

$$\text{ESI}(\%) = \frac{A_{15}}{A_0} \times 100 \quad (5)$$

A_0 represents the absorbance of the sample measured at 0 min, N denotes the dilution factor, C is the concentration of the sample, φ indicates the volume fraction of the oil phase, and A_{15} is the absorbance of the sample measured at 15 min.

2.6. Thermal stability

The samples were sealed in aluminum pans and heated from 25 °C to 220 °C at a rate of 10 °C/min under a constant nitrogen purge (30 mL/min) using a differential scanning calorimeter (DSC-3, Mettler Toledo, Switzerland).

2.7. Ability of β-Lg-4MBQ covalent conjugates to stabilize β-carotene emulsions

2.7.1. β-carotene emulsions preparation

Aqueous phase of β-Lg and β-Lg-4MBQ conjugates were prepared at a concentration of 30 mg/mL in phosphate buffer (10 mmol/L, pH 7.0). The oil phase was prepared by dispersing β-carotene (0.1 %, *w*/w) in soybean oil and sonicated at 50 °C for 25 min until the β-carotene was completely dissolved. The water and oil phases were then mixed in a mass ratio of 9.5:0.5 and homogenized for 2 min at 20,000 r/min using a high-speed homogenizer. The resulting coarse emulsion was further homogenized by ultrasonication at 40 MPa for 5 min in an ice-water bath, with 5 s of action followed by 5 s of interval.

2.7.2. Particle size, ζ-potential measurements

The obtained emulsions were diluted 100 times with phosphate buffer (10 mmol/L, pH 7.0). Then their particle size and ζ-potential were measured by the method mentioned in 2.3.7.

2.7.3. β-carotene retention

β-Carotene emulsion was taken in a centrifuge tube, and an ethanol/n-hexane mixed organic solution (2:3, *v*/v) was added for extraction at a volume ratio of 2:25. The extraction was repeated with n-hexane, and the upper layers of the extracts were combined. The β-carotene content was measured at 450 nm using UV–Vis spectrophotometer.

2.7.4. Thiobarbituric acid-reactive substances (TBARS)

TBARS concentration was measured according to the method described in previous study (Dimakou & Oreopoulou, 2012). A volume of 250 μL of emulsion was mixed with 500 μL of TBA solution. The mixture was then incubated in a boiling water bath for 30 min. After cooling to 25 °C, the mixture was filtered through a 0.45 μm syringe filter. The absorbance was measured at 532 nm and the concentration of TBARS in the emulsion was determined using a standard curve of 1,1,3,3-tetraethoxypropane.

2.7.5. Chemical and storage stability of β-carotene emulsions

2.7.5.1. Thermal stability. Freshly prepared β-carotene emulsions were placed in brown bottles, incubated at 50 °C, 60 °C, 70 °C, 80 °C and 90 °C for 30 min, and then quickly cooled down to 25 °C. The particle size, ζ-potential, and β-carotene retention were analyzed as mentioned in 2.7.2 and 2.7.3. The TBARS value of emulsions incubated at 90 °C for 30 min was measured according to 2.7.4.

2.7.5.2. Natural light stability. Freshly prepared β-carotene emulsions were placed in transparent bottles and exposed to natural light for 8 h. The particle size, ζ-potential, and β-carotene retention were analyzed at 0 h, 2 h, 4 h, 6 h and 8 h as mentioned in 2.7.2 and 2.7.3. The TBARS value of emulsions exposed to natural light for 8 h was measured according to 2.7.4.

2.7.5.3. Storage stability. Freshly prepared β-carotene emulsions were stored at 4 °C for 15 days in dark, and the retention of β-carotene in the emulsions were analyzed at 0 d, 3 d, 6 d, 9 d, 12 d, and 15 d as mentioned in 2.7.3. The TBARS value of emulsions stored at 4 °C for 15 d was measured according to 2.7.4.

2.8. Statistical data analysis

All experiments were conducted in triplicate, with results expressed as means ± standard deviations. Significant differences ($P < 0.05$) were evaluated using Duncan's multiple range test in SPSS 26.

3. Results and discussion

3.1. Total polyphenol, free sulfhydryl and amino groups content

4MBQ can form covalent bonds with cysteine, lysine, arginine, and histidine residues in β-Lg, with cysteine residues being the primary sites of their covalent interaction (Li et al., 2024). β-Lg-4MBQ-0.2, β-Lg-4MBQ-0.4, and β-Lg-4MBQ-0.8 were prepared with molar ratios of 4MBQ to β-Lg free thiols at 1:2, 1:1, and 2:1, respectively. The total polyphenol content of β-Lg-4MBQ-0.2, β-Lg-4MBQ-0.4 and β-Lg-4MBQ-0.8 was 16.14 ± 0.30, 16.83 ± 0.22, and 19.04 ± 0.17 mg/g, respectively, as shown in Table 1. The reactive groups in β-Lg capable of covalent reactions with 4MBQ include fifteen lysine, three histidine, three arginine residues, and one free thiol group. These groups outnumber the 4MBQ molecules available. As a result, increasing the concentration of 4MBQ leads to an increase in the participation of β-Lg's active groups in reactions, and consequently, the total phenolic content in the β-Lg-4MBQ conjugates significantly rises with higher 4MBQ additions.

The concentrations of free sulfhydryl and amino groups in β-Lg-4MBQ conjugates were significantly lower than those in native β-Lg ($P < 0.05$, Table 1). Similar reductions were observed in the covalent interaction between chlorogenic acid, EGCG, and gallic acid with β-Lg (Man et al., 2024), and in the covalent binding of gallic acid and protocatechuic acid with whey protein (Fei et al., 2023). These findings suggest that covalent bonds formed between 4MBQ and the free sulfhydryl and amino groups in β-Lg. As the concentration of 4MBQ increased, significant reductions in both free sulfhydryl and amino groups were observed, demonstrating that their engagement in reactions with β-Lg intensified with greater additions of 4MBQ. However, at molar concentration ratios of 4MBQ to β-Lg's free sulfhydryl groups of 1:1 (β-Lg-4MBQ-0.4) and 2:1 (β-Lg-4MBQ-0.8), the levels of free sulfhydryl groups in the conjugates were 18.46 ± 0.21 and 17.12 ± 0.18 μmol/g, respectively, both approximately 50 % of those found in native β-Lg. The substantial retention of sulfhydryl content might be attributed to the markedly higher proportions of lysine, histidine, and tryptophan residues relative to free sulfhydryl groups in β-Lg.

3.2. Sites identification for the reaction between β-Lg and 4MBQ

Forty-three peptides with covalent bindings to 4MC at twenty unique amino acid sites were characterized in β-Lg-4MBQ-0.4, as shown in Table 2. Furthermore, in β-Lg-4MBQ-0.4, 4MBQ was observed to react with 14 lysine, 3 arginine, 2 histidine, and 1 free cysteine residues of β-Lg.

This demonstrates that at a molar concentration ratio of 1:1 between 4MBQ and β-Lg's free sulfhydryl groups, all types of reactive amino acid residues in β-Lg participate in the reaction with 4MBQ. This observation is consistent with the significantly lower concentrations of both free thiol and amino groups in the β-Lg-4MBQ conjugates compared to native β-Lg. In our previous study, we have identified β-Lg-4MBQ conjugates formed at molar ratios of 4MBQ to β-Lg free thiols of 1:2 (β-Lg-4MBQ-0.2) and 2:1 (β-Lg-4MBQ-0.6) (Li et al., 2024). As the molar concentration ratio of 4MBQ to β-Lg free thiols increases, the number of peptide sequences in β-Lg covalently bound to 4MBQ correspondingly increases.

Table 2
Covalent binding sites detected in β-Lg-4MBQ-0.4 by trypsin, chymotrypsin or GluC digestion.

No.	Theoretical molecular weight (Da)	Experimental molecular weight (Da)	Peptide sequence	*m/z*
1	1064.18	1064.53	VAGTW***H***(20)SLA	533.3
2	1988.97	1988.97	QKWENGECAQ***K***(69)***K***(70)IIA	664.0
3	2102.05	2102.05	LQKWENGECAQ***K***(69)***K***(70)IIA	1052
4	1353.64	1353.64	LACQCLV***R***(124)TPE	677.8
5	1111.51	1111.52	ACQCLV***R***(124)TP	556.8
6	1270.61	1270.61	CQ***C***(121)LVRTPEV	636.3
7	1572.88	1572.88	IIAE***K***(75)T***K***(77)IPAVF	787.4
8	2417.69	2417.28	AL***K***(141)ALPM***H***(146)I***R***(148)LAFNPTQL	806.8
9	1350.42	1350.68	ILLQ***K***(60)WENGE	676.3
10	2914.58	2914.59	ECAQKKIIAEKT***K***(77)IPAVF***K***(83)IDALN	972.5
11	1242.61	1242.62	VTQTM***K***(8)GLDI	622.3
12	1113.54	1113.54	VTQTM***K***(8)GLD	557.8
13	1324.71	1324.71	TM***K***(8)GLDIQKVA	663.4
14	1224.60	1224.60	LACQCLV***R***(124)TP	613.3
15	1236.52	1236.67	LPM***H***(146)IRLAF	413.2
16	1218.42	1218.66	LPMHI***R***(148)LAF	407.2
17	1726.91	1726.91	LVLDTDY***K***(100)***K***(101)YLL	864.5
18	1068.23	1068.53	Q***C***(121)LVRTPE	535.3
19	993.10	993.49	VAGTW***H***(20)SL	497.8
20	1243.62	1243.62	***K***(14)VAGTW***H***(20)SL	415.5
21	1452.64	1452.71	LACQCLV***R***(124)TPEV	727.4
22	1691.87	1691.84	TQTM***K***(8)GLDIQ***K***(14)VA	565.0
23	1174.22	1175.59	ECAQ***K***(69)***K***(70)II	588.8
24	1052.57	1052.57	I***R***(148)LAFNPT	527.3
25	1324.49	1324.61	W***H***(20)SLAMAASDI	663.3
26	1589.72	1589.71	DY***K***(100)KYLLFCME	795.9
27	1476.78	1476.79	ALE***K***(135)FD***K***(138)ALKA	493.3
28	1249.66	1249.66	IDALNEN***K***(91)VL	625.8
29	1288.58	1288.59	LDTDY***K***(100)***K***(101)Y	430.5
30	2568.26	2568.26	TQTM***K***(8)GLDIQ***K***(14)VAGTW***H***(20)SLA	857.1
31	1560.79	1560.79	GECAQ***K***(69)***K***(70)IIAEK	781.4
32	1269.39	1269.70	L***R***(40)VYVEELK	424.2
33	1512.69	1512.69	TW***H***(20)SLAMAASDIS	505.2
34	1467.69	1467.69	PEQSLACQCLV***R***(124)	734.8
35	1517.92	1517.92	QKKIIAE***K***(75)TKIP	760.0
36	1123.59	1123.59	D***K***(138)ALKALPM	375.5
37	1337.64	1337.64	VAGTW***H***(20)SLAMAA	669.8
38	1762.92	1762.92	LE***K***(135)FDKAL***K***(141)ALPM	882.5
39	1579.82	1579.82	PAVF***K***(83)IDALNENK	790.9
40	1791.97	1791.98	PAVF***K***(83)IDALNENKVL	598.3
41	2118.04	2118.05	***K***(60)WENGECAQ***KK***(70)IIAEK	707.0
42	1679.83	1679.83	DALNEN***K***(91)VLVLDTD	840.9
43	1661.82	1661.82	LDTDY***K***(100)***K***(101)YLLF	416.5

Table 1
The total polyphenol, free sulfhydryl group and free amino group content, H_0, and color metrics of β-Lg and β-Lg-4MBQ covalent conjugates.

Sample	Total polyphenol (mg/g)	Free sulfhydryl group (μmol/g)	Free amino group (μmol/g)	H_0	L*	a*	b*	△E
β-Lg	–	35.31 ± 0.48$^{a\#}$	265.58 ± 4.86^{a}	698.27 ± 8.28^{c}	61.26 ± 0.29^{a}	−0.34 ± 0.01^{c}	1.57 ± 0.02^{d}	–
β-Lg-4MBQ-0.2	16.14 ± 0.30^{c}	19.11 ± 0.21^{b}	215.39 ± 5.32^{b}	792.55 ± 13.47^{b}	56.02 ± 0.05^{b}	−0.32 ± 0.02^{c}	4.04 ± 0.02^{c}	5.80 ± 0.06^{c}
β-Lg-4MBQ-0.4	16.83 ± 0.22^{b}	18.46 ± 0.21^{c}	175.49 ± 2.55^{c}	943.97 ± 8.92^{a}	48.47 ± 0.04^{c}	0.31 ± 0.01^{b}	5.87 ± 0.02^{b}	13.52 ± 0.04^{b}
β-Lg-4MBQ-0.8	19.04 ± 0.17^{a}	17.12 ± 0.18^{d}	181.28 ± 5.37^{c}	935.38 ± 3.80^{a}	37.91 ± 0.14^{d}	0.69 ± 0.02^{a}	6.00 ± 0.10^{a}	23.79 ± 0.75^{a}

Note: $^{\#}$Free sulfhydryl group content of β-Lg was obtained from our previous study (Li et al., 2024). Different superscript lowercase letters indicate significant differences between different samples ($P < 0.05$).

Specifically, 29 peptide sequences were identified at a ratio of 1:2 (β-Lg-4MBQ-0.2), 43 sequences at 1:1 (β-Lg-4MBQ-0.4), and 55 sequences at 2:1 (β-Lg-4MBQ-0.8). This indicates that with the increasing concentration of 4MBQ, the probability of active groups in β-Lg participating in the reaction significantly increases. The results from section 3.1 have supported this, showing that higher quinone content corresponds to a gradual decrease in the free amine and thiol content in the covalent adducts.

Similarly, when the molar concentration ratios of 4MBQ to β-Lg free thiols were 1:1 and 2:1, the number of amino acid residue sites in β-Lg involved in covalent reactions with 4MBQ was greater than at a molar ratio of 1:2. Specifically, at a ratio of 1:2, 17 sites were identified, while at ratios of 1:1 and 2:1, 20 sites were identified (Li et al., 2024). In the study by Liu et al., 10 lysine residues, 1 histidine residue, 1 arginine residue, and 2 cysteine residues in β-Lg were identified to participate in covalent interactions with 4MBQ (J. Liu et al., 2024). In addition, Waqar et al. (2022) reported that 11 lysine residues, 4 cysteine residues, 2 histidine residues, 1 arginine residue, and 1 tryptophan residue in β-Lg were involved in covalent interactions with 4MBQ.These variations may be due to differences in reaction conditions or the quantities of reactants used. The secondary mass spectra of representative peptide segments 18, 19, 28, and 32, as listed in Table 2, are depicted in Fig. 1a-1d. Conjugates formed from the reaction of 4MBQ with lysine and arginine residues in β-Lg exhibited an amine-quinone structure, while those formed with histidine and cysteine residues displayed a phenol structure. These observations align with our previous research findings (Li et al., 2024).

3.3. UV–vis and fluorescence analysis of β-Lg-4MBQ conjugates

As shown in Fig. 2a, β-Lg exhibits a characteristic absorption peak at 277 nm, attributed to the conjugated double bond in tyrosine and tryptophan residues (Xu, Hao, Sun, & Tang, 2019). The UV absorbance values of β-Lg-4MBQ-0.2 and β-Lg-4MBQ-0.4 at 277 nm showed no significant difference compared to that of β-Lg. However, the absorbance value at 277 nm for β-Lg-4MBQ-0.8 was significantly higher than that of β-Lg. The results from section 3.2 indicated that as the concentration of 4MBQ increased, a greater number of amino acid residues in β-Lg participate in the reaction. This leads to changes in the microenvironment surrounding the aromatic amino acid residues and alterations in the protein conformation (D. Wang, Li, Hou, Zhang, & Li, 2024),

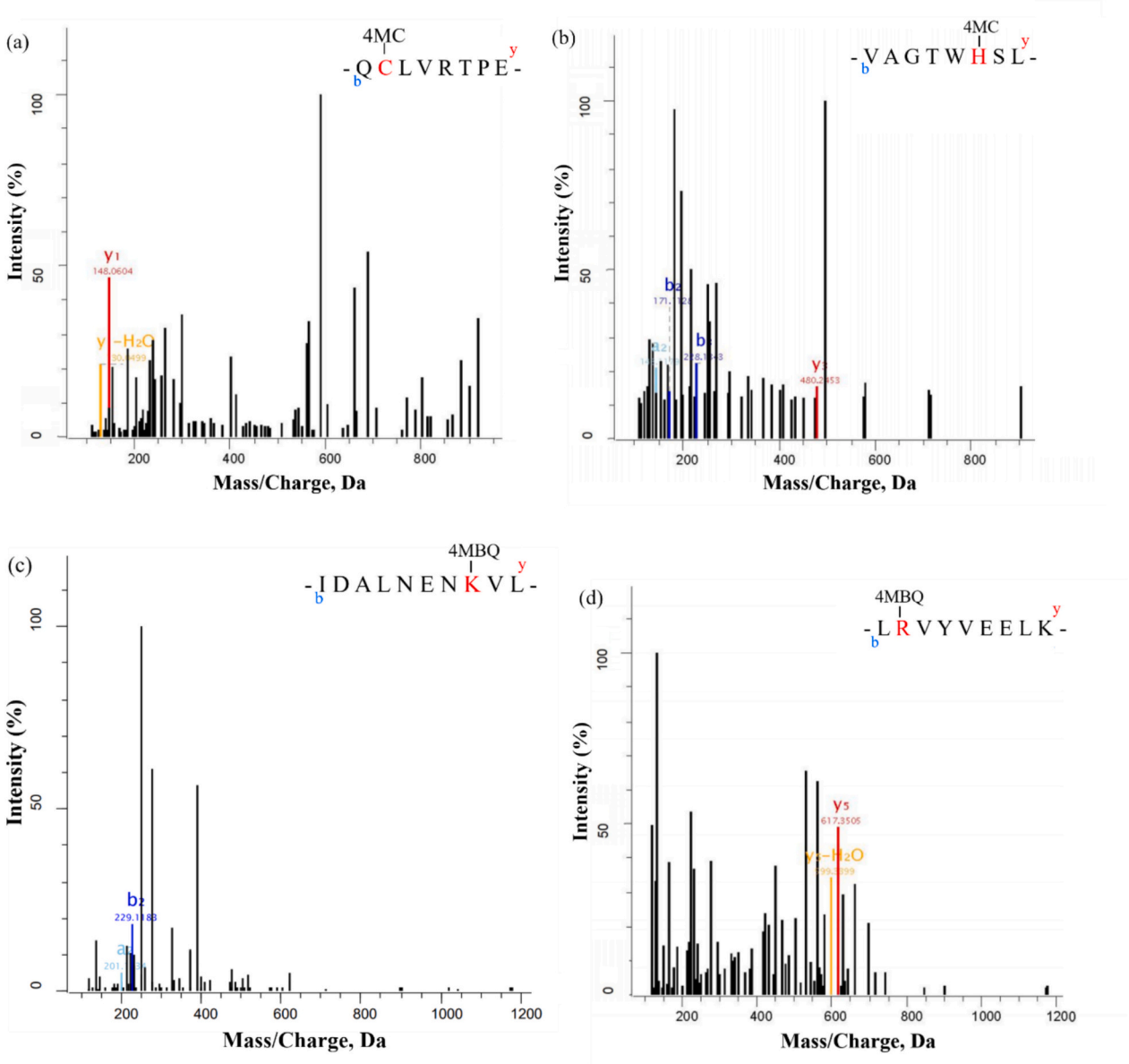

Fig. 1. MS/MS spectra of peptide 18 (a), peptide 19 (b), peptide 28 (c), and peptide 32 (d) illustrated in Table 2.

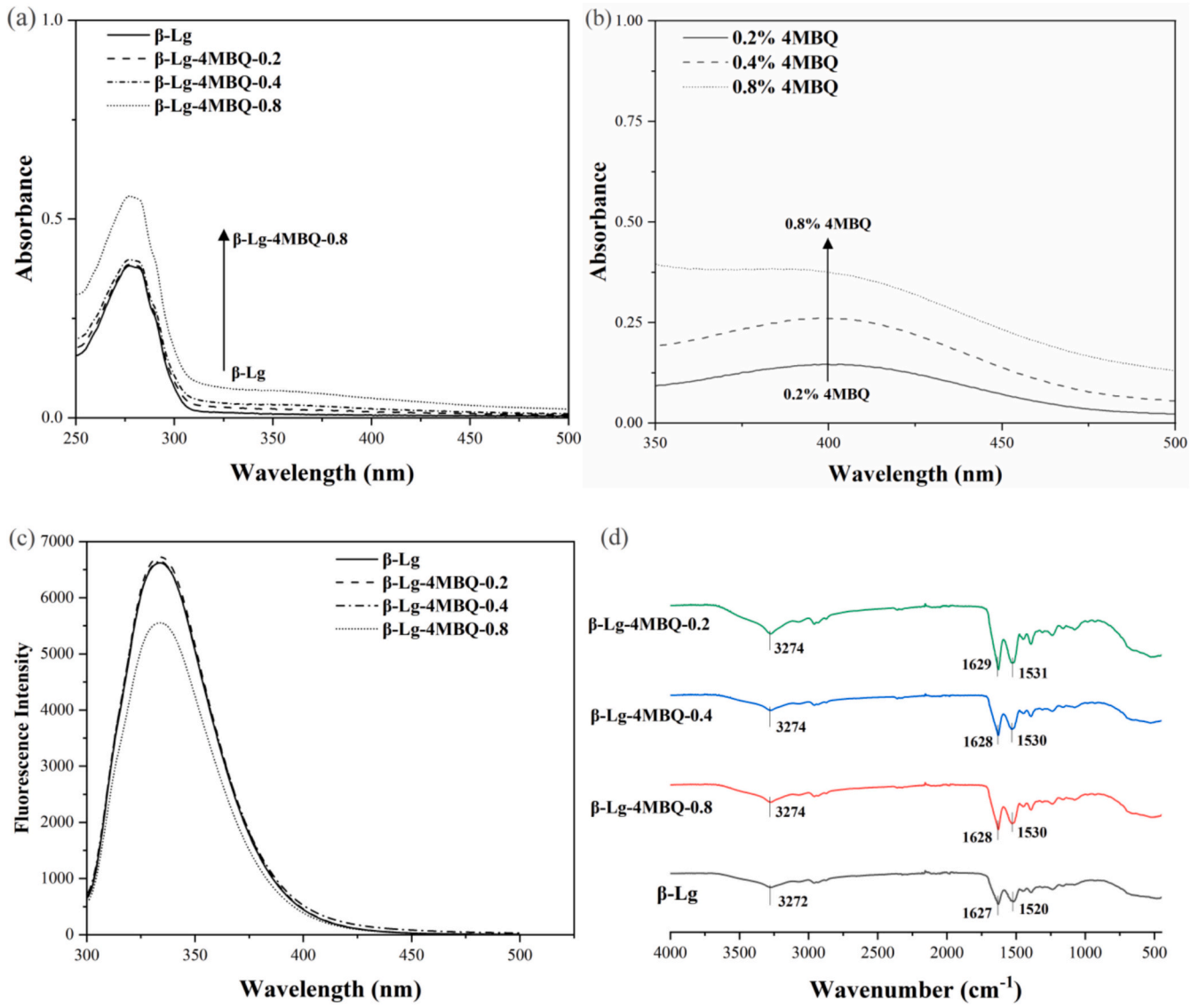

Fig. 2. The UV–Vis (a), fluorescence (c), and ATR-FTIR (d) spectra of β-Lg, β-Lg-4MBQ-0.2, β-Lg-4MBQ-0.4 and β-Lg-4MBQ-0.8, and UV–Vis spectrum (b) of 4MBQ.

resulting in variations in the UV absorption. Similar UV absorption variations were also noted in the non-covalent interactions between rutin and β-Lg (Al-Shabib et al., 2018). The characteristic absorption wavelength of 4MBQ is 401 nm (Li et al., 2016), with absorbance values approximately 0.37 for 0.8 % 4MBQ, 0.26 for 0.4 % 4MBQ, and 0.15 for 0.2 % 4MBQ (Fig. 2b). Upon reacting with β-Lg, 4MBQ was depleted, resulting in the disappearance of its characteristic absorption at 401 nm. Thus, the absorbance of β-Lg-4MBQ conjugates at 401 nm consistently remains below 0.05 (Fig. 2a).

The intrinsic fluorescence of β-Lg, primarily generated by its tryptophan and tyrosine residues when excited at 280 nm, serves as a sensitive method for assessing alterations in protein conformation (Simion et al., 2015). As depicted in Fig. 2c, the fluorescence intensities of β-Lg-4MBQ-0.2 and β-Lg-4MBQ-0.4 are comparable to that of β-Lg, while the fluorescence intensity of β-Lg-4MBQ-0.8 is significantly reduced relative to β-Lg. The interaction between 4MBQ and β-Lg did not affect the maximum emission wavelength of the protein. As mentioned in 3.2, tryptophan and tyrosine residues in β-Lg were not the target for the reaction with 4MBQ. The degree of participation of β-Lg amino acid residues in reactions increases with increasing concentrations of 4MBQ. At a molar ratio of 2:1 between 4MBQ and β-Lg free thiols, the covalent interactions between quinones and amino acid residues significantly alter the polarity in the vicinity of the fluorescent groups, resulting in a substantial decrease in fluorescence intensity (Fei et al., 2023). The diminished fluorescence intensity resulting from the reaction between 4MBQ and β-Lg could also be attributed to modifications in the protein's secondary structure (Han, Liang, Tian, Liu, & Wang, 2022).

3.4. *ATR-FTIR and CD analysis of β-Lg-4MBQ conjugates*

Fig. 2d presents the ATR-FTIR spectrum of β-Lg, which displays three distinct peaks at 3272 cm^{-1}, 1627 cm^{-1}, and 1520 cm^{-1}. These peaks correspond to the amide A, I, and II bands, respectively. Specifically, the amide A band is associated with N—H and hydrogen bond stretching vibrations. The amide I band arises from C═O stretching vibrations, and the amide II band involves N—H bending and C—N stretching vibrations (L. Zhang et al., 2018). The β-Lg-4MBO covalent adduct showed no significant shift in the amide A and I bands when compared to β-Lg. Nevertheless, the amide II band exhibited a red shift from 1520 cm^{-1} to 1531 cm^{-1}, indicative of the formation of new C—N bonds in β-Lg-4MBQ conjugates (Jing et al., 2020). These new C—N bonds are formed by the reaction of 4MBQ with the lysine, arginine, and histidine residues of β-Lg (Li et al., 2024), which aligns with the site identification results discussed in Section 3.2. The intensity of the amide A bands in β-Lg-

4MBQ-0.8 was elevated compared to that in β-Lg. This is related to the reaction of β-Lg histidine and cysteine residues with 4MBQ, which introduces phenolic hydroxyl groups, as the reaction products of histidine and cysteine residues with 4MBQ exist in the form of phenolic structures (Li et al., 2024). The intensity of amide I and II in β-Lg-4MBQ-0.8 also higher than that of β-Lg, indicating that the changed of β-Lg's secondary structure and the vigorous stretching vibrations of C—N (Yan et al., 2021). Similar phenomenon was observed in the FTIR spectrum of soy protein hydrolysates-EGCG conjugates (Wu, Lin, Zhang, Wang, & Ding, 2023).

The secondary structure changes of β-Lg and β-Lg-4MBQ conjugates were determined by CD spectroscopy. The contents of α-helices, β-sheets, β-turns, and random coils were calculated using CDNN software, as shown in Table 3. As the concentration of 4MBQ in the reaction system increases from 0.0 % to 0.8 %, the content of α-helices in β-Lg decreases from 17.46 ± 0.24 % to 16.20 ± 0.23 %, and the β-sheet content increases from 30.62 ± 0.30 % to 32.10 ± 0.19 %. These changes indicate that the addition of 4MBQ alters the secondary structure of β-Lg, leading to a transition from α-helices to β-sheets, rather than reducing the overall order of the structure (i.e., the content of α-helices and β-sheets). This is similar to the trend of secondary structure changes after α-lactalbumin is covalently bound with chalconoids (Jiang et al., 2020).

3.5. Particle size and ζ-potential of β-Lg-4MBQ conjugates

The particle size and polydispersity index (PDI) of β-Lg and β-Lg-4MBQ conjugates were shown in Table 3. It was observed that the particle size of β-Lg and its conjugates with 4MBQ did not undergo significant changes ($P > 0.05$) as the concentration of 4MBQ increased. This lack of significant change can be partly attributed to the relatively minor impact of the 4MBQ covalent interactions on the molecular weight of β-Lg. Specifically, each interaction between 4MBQ and an amino acid residue results in an increase in molecular weight of approximately 120 Da, a negligible amount compared to the overall molecular weight of β-Lg (18.3 KDa). Furthermore, the total polyphenol content of the β-Lg-4MBQ conjugates ranged from 16 to 19 mg/g of the sample. Consequently, the modest increase in molecular weight due to 4MBQ conjugation does not significantly affect the particle size of the β-Lg. This is consistent with findings from a previous study, which demonstrated that under neutral conditions, the non-covalent complexes between egg white protein (EWP) and tea polyphenols did not exhibit significant differences in particle size compared to EWP alone (Sun et al., 2022). The PDI of β-Lg-4MBQ-0.2 and β-Lg-4MBQ-0.4 was significantly smaller than that of β-Lg and β-Lg-4MBQ-0.8. A lower PDI indicates a more uniform distribution of particle sizes. The covalent interaction between EGCG and soy protein hydrolysates (SPHs) resulted in an increase in the particle size of SPHs (Wu et al., 2023). Conversely, both covalent and non-covalent interactions of gallic acid with pea protein isolate (PPI) led to a decrease in the particle size of PPI (M. Zhang, Fan, Liu, & Li, 2023). These divergent outcomes may be ascribed to differences in the types of polyphenols and proteins utilized, as well as the experimental conditions employed.

The surface charge of β-Lg and β-Lg-4MBQ conjugates were in the order of β-Lg-4MBQ-0.8 ≈ β-Lg-4MBQ-0.4 > β-Lg-4MBQ-0.2 > β-Lg at pH 7.0 (Table 3). A higher surface charge on proteins enhances the repulsive interactions among proteins, aiding in maintaining their dispersion within the solution and thereby contributing to the overall stability of the solution (Chi, Krishnan, Randolph, & Carpenter, 2003). With the increase in 4MBQ concentration, there was a corresponding rise in the surface charge of the covalent conjugates. This increase is attributed to the reaction between 4MBQ and β-Lg, which leads to the consumption of the protein's free amino groups and the incorporation of phenolic hydroxyl groups (Pham, Wang, Zisu, & Adhikari, 2019). This mechanism is corroborated by the observed trends in the conjugates' total phenolic content and free amino group levels (Table 1), which increase and decrease, respectively, with rising concentrations of 4MBQ.

3.6. Antioxidant activity of β-Lg-4MBQ conjugates

The antioxidative properties of β-Lg, both before and after its reaction with 4MBQ, were assessed through its ability to scavenge DPPH and ABTS radicals. As depicted in Fig. 3a, the covalent conjugates of β-Lg with 4MBQ demonstrated a significantly enhanced capacity for scavenging these radicals, compared to the native protein. Furthermore, there was a significant increase ($P < 0.05$) in antioxidant ability as the concentration of 4MBQ increased, with the effectiveness ranked as follows: β-Lg-4MBQ-0.8 > β-Lg-4MBQ-0.4 > β-Lg-4MBQ-0.2 > β-Lg. This trend is consistent with the observed increase in the total phenolic content of the conjugates as the concentration of 4MBQ rises (Table 1). This suggests that higher concentrations of 4MBQ lead to more reactive groups within the β-Lg residues becoming involved, which results in an increase in the incorporation of phenolic hydroxyl groups (Li et al., 2024). These groups are capable of donating hydrogen atoms, effectively quenching radicals present in the system. These results were consistent with findings from some prior research. Specifically, Fei et al. (2023) reported enhanced antioxidant activity in whey protein following covalent attachment to protocatechuic acid and gallic acid. Man et al. (2024) observed similar enhancements in the antioxidant properties of β-Lg when it was covalently bound with tea polyphenols.

3.7. H_0 and emulsifying activity of β-Lg-4MBQ conjugates

H_0 critically influences the interfacial behaviors of proteins, particularly their emulsification and foaming properties (Man et al., 2024). The H_0 of the β-Lg-4MBQ conjugates was significantly higher than that of native β-Lg and increases with the concentration of 4MBQ. Specifically, the H_0 values were as follows: β-Lg-4MBQ-0.8 (935.97 ± 3.80) ≈ β-Lg-4MBQ-0.4 (943.97 ± 8.92) > β-Lg-4MBQ-0.2 (792.55 ± 13.47) > β-Lg (698.27 ± 8.28). There was a significant increase in β-sheet content of β-Lg-4MBQ conjugates compared to native β-Lg (Table 2). This elevation in β-sheets facilitates the exposure of the protein's hydrophobic regions (G. Liu et al., 2022). In addition, the reaction of β-Lg with 4MBQ leads to the introduction of hydrophobic phenyl groups (Ke & Li, 2024). The covalent conjugates formed between ferulic acid and β-Lg also demonstrated an increased H_0 compared to β-Lg alone (Xue et al., 2023).

EAI and ESI are important indicators that characterize the emulsifying properties of proteins. They reflect the ability of proteins to form an emulsifying layer at the oil-water interface and the stability of the

Table 3
The secondary structure content, ζ-potential, particle size and PDI of β-Lg and β-Lg-4MBQ covalent conjugates.

Sample	α-Helix (%)	β-Sheet (%)	β-Turn (%)	Random coil (%)	ζ-potential(mV)	Particle size(nm)	PDI (%)
β-Lg	17.46 ± 0.24^{a}	30.62 ± 0.30^{b}	18.47 ± 0.11^{a}	33.45 ± 0.13^{a}	−15.30 ± 0.10^{c}	218.01 ± 20.83^{a}	20.83 ± 1.36^{b}
β-Lg-4MBQ-0.2	16.64 ± 0.17^{b}	31.79 ± 0.30^{a}	18.65 ± 0.13^{a}	33.05 ± 0.25^{a}	−17.30 ± 0.70^{b}	198.33 ± 17.83^{a}	17.83 ± 0.35^{c}
β-Lg-4MBQ-0.4	16.46 ± 0.18^{bc}	32.07 ± 0.33^{a}	18.73 ± 0.12^{a}	32.84 ± 0.21^{a}	−18.23 ± 0.25^{a}	216.08 ± 18.67^{a}	18.67 ± 0.74^{c}
β-Lg-4MBQ-0.8	16.20 ± 0.23^{c}	32.10 ± 0.19^{a}	18.18 ± 0.65^{a}	33.52 ± 0.75^{a}	−18.47 ± 0.38^{a}	227.08 ± 26.97^{a}	26.97 ± 1.39^{a}

Note: Different superscript lowercase letters indicate significant differences between different samples ($P < 0.05$).

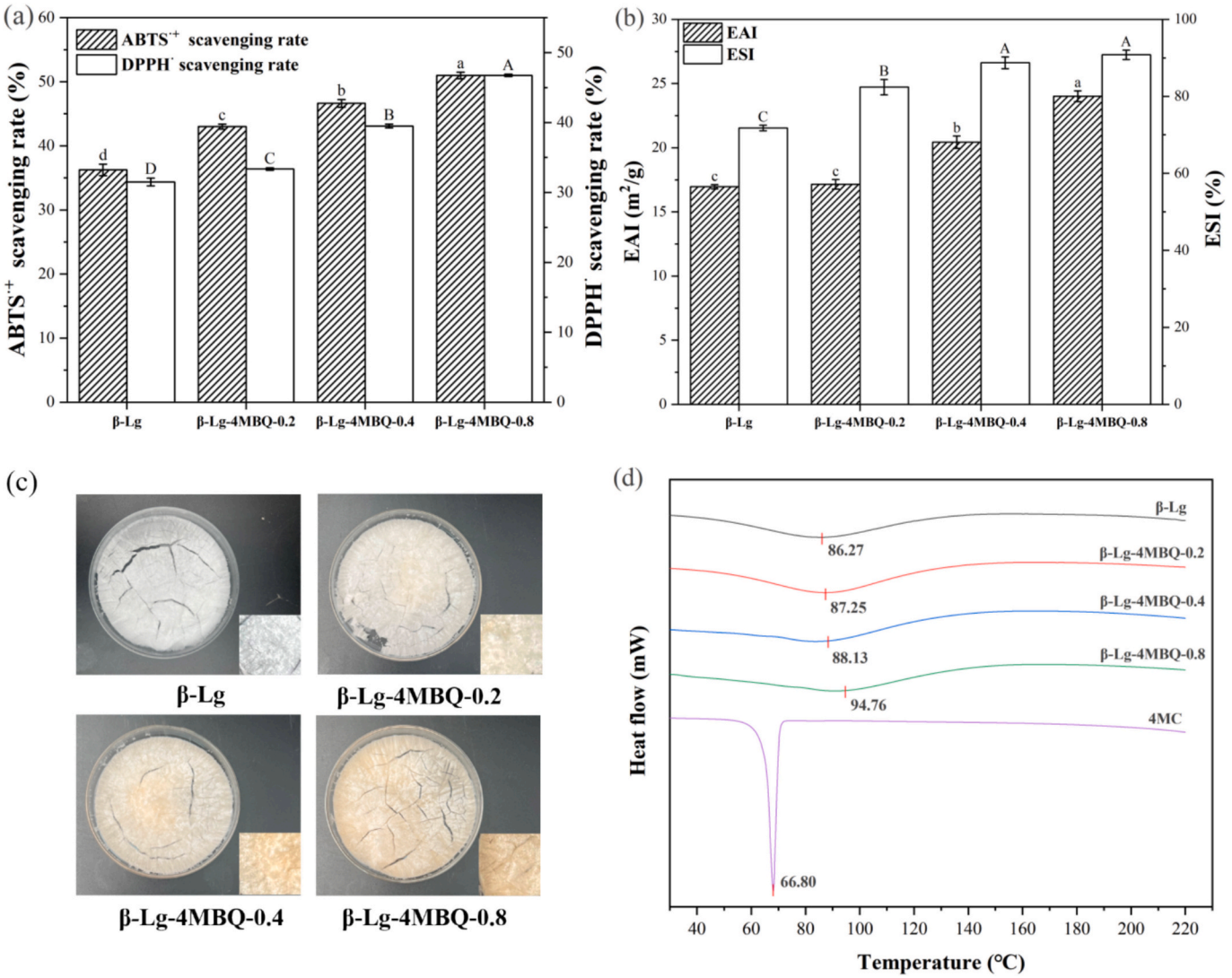

Fig. 3. The ABTS and DPPH scavenging rate (a), EAI and ESI (b), photograph (c) and DSC spectra (d) of β-Lg, β-Lg-4MBQ-0.2, β-Lg-4MBQ-0.4 and β-Lg-4MBQ-0.8. Different letters indicate significant differences between different emulsifiers ($P < 0.05$).

emulsion formed (Fei et al., 2023). The ESI for the β-Lg-4MBQ conjugates is significantly greater than that of native β-Lg ($P < 0.05$). In terms of EAI, β-Lg-4MBQ-0.8 and β-Lg-4MBQ-0.4 showed significantly enhanced values relative to native β-Lg ($P < 0.05$), whereas β-Lg-4MBQ-0.2 did not differ significantly from native β-Lg in EAI ($P > 0.05$). Specifically, the order for ESI among the β-Lg and its conjugates with 4MBQ was: β-Lg-4MBQ-0.8 (90.79 % ± 1.23 %) ≈ β-Lg-4MBQ-0.4 (88.73 % ± 1.53 %) > β-Lg-4MBQ-0.2 (82.40 % ± 1.99 %) > β-Lg (71.79 % ± 0.72 %), and for EAI, it was: β-Lg-4MBQ-0.8 (24.01 ± 0.42 m^2/g) > β-Lg-4MBQ-0.4 (20.43 ± 0.48 m^2/g) > β-Lg-4MBQ-0.2 (17.15 ± 0.37 m^2/g) ≈ β-Lg(16.96 ± 0.16 m^2/g). These trends were similar to the observed changes in the H_0. After reacting with 4MBQ, there was an observed increase in β-sheet content and a corresponding decrease in α-helix content within the secondary structure of β-Lg (Table 3), suggesting a partial unfolding of the protein (G. Liu et al., 2022). Moreover, the increased β-sheet content coupled with the reduced α-helix content enhances the protein's flexibility, which promotes protein rearrangement at the oil-water interface (G. Liu et al., 2022). All these contribute to the improving of emulsifying properties of the protein. Furthermore, the reaction of 4MBQ with protein may alter the interactions among proteins, resulting in an increase in steric hindrance and electrostatic repulsion between droplets (D. Wang et al., 2024). These changes decrease the interfacial tension at the oil-water boundary, thereby preventing droplet aggregation (D. Wang et al., 2024). Consequently, the EAI and ESI of the β-Lg-4MBQ conjugates showed a positive correlation with the concentration of 4MBQ. Under neutral conditions, the non-covalent complexes formed between tea polyphenols and EWP demonstrated significantly higher EAI and ESI compared to the native EWP (Sun et al., 2022). However, the ESI of these complexes showed a positive correlation with the amount of tea polyphenols added, whereas the EAI exhibits a negative correlation. Therefore, the emulsifying properties of the interaction products between polyphenols and proteins may be related to differences in polyphenol, protein, and the conditions of their interaction.

3.8. Color of β-Lg-4MBQ conjugates

As depicted in Fig. 3c, there is a noticeable color differentiation between the β-Lg-4MBQ conjugates and β-Lg. The ΔE values (Table 1), indicative of color differences, were sequenced as follows: β-Lg-4MBQ-0.8 > β-Lg-4MBQ-0.4 > β-Lg-4MBQ-0.2. This pattern indicates that the colorimetric disparity between the reaction products of 4MBQ with β-Lg and the native protein becomes increasingly pronounced as the concentration of 4MBQ rises. Specifically, increasing concentrations of 4MBQ led to a noticeable decline in the L* value, while the a* and b* values of the β-Lg-4MBQ conjugates increased. This phenomenon is

attributed to the incorporation of polyphenols, which modify the optical properties of the protein by altering light absorption and/or scattering and increasing of chromophores to absorb light (T. Dai et al., 2020; McClements, 2002). As a result, these covalent adducts absorb more light and reflect less, leading to a darker appearance. Furthermore, higher concentrations of 4MBQ result in greater involvement of lysine residues from β-Lg in the reaction, promoting the formation of increased red amine-quinone product (Li et al., 2016). This leads to enhanced selective light wave absorption by the chromophores (T. Dai et al., 2020), correspondingly elevating the a and b values as the 4MBQ concentration increases.

3.9. Thermal stability of β-Lg-4MBQ conjugates

As shown in Fig. 3d, the denaturation temperature (T_d) of β-Lg and 4MC were 86.27 °C and 66.80 °C, respectively. The thermal stability of β-Lg-4MBQ conjugates was superior to that of β-Lg and 4MC. Furthermore, it increased with higher 4MBQ content in the following order: β-Lg-4MBQ-0.8 (94.76 °C) > β-Lg-4MBQ-0.4 (88.13 °C) > β-Lg-4MBQ-0.2 (87.25 °C). The steric hindrance in β-Lg-4MBQ conjugates significantly reduces protein aggregation, thereby enhancing their thermal stability (Ke et al., 2024). As the number of polyphenols covalently grafted onto β-Lg increases, the steric hindrance may intensify, thereby strengthening the thermal stability of the β-Lg-4MBQ conjugates. This is consistent with the results reported by Fei et al. (2023), showing that the thermal stability of the covalent conjugates formed by the interaction between gallic acid/protocatechuic acid and whey protein was higher than that of the original whey protein.

3.10. Characterization of β-carotene emulsion stabilized by β-Lg-4MBQ conjugates

β-Carotene, the predominant carotenoid in dietary sources, is an essential precursor to vitamin A and a key antioxidant. It is commonly used in food processing to enhance both the nutritional value and coloration of food products. However, due to its limited water solubility and susceptibility to degradation under heat and light exposure (Lino et al., 2020), its application in food systems is often constrained. The use of β-Lg-4MBQ conjugates as antioxidant emulsifiers in water-in-oil emulsions could enhance the stability and broaden the application of β-carotene in food products.

3.10.1. Particle size and ζ-potential

Particle size is a critical parameter influencing emulsion stability. β-Carotene stabilized by β-Lg-4MBQ conjugates exhibited significantly smaller particle sizes compared to those stabilized by native β-Lg. Specifically, the particle sizes were as follows: β-Lg (395.27 ± 3.34 nm) > β-Lg-4MBQ-0.8 (347.05 ± 6.14 nm) > β-Lg-4MBQ-0.2 (329.87 ± 9.53 nm) > β-Lg-4MBQ-0.4 (308.33 ± 6.79 nm). The decrease in particle size may be attributed to the enhanced interfacial activity and adsorption of the protein following its reaction with 4MBQ (Huang, Xia, Liu, & Wang, 2024). Emulsions stabilized by conjugates formed through the covalent interaction of soybean meal hydrolysate with EGCG, proanthocyanidin, gallic acid, or caffeic acid also exhibited smaller particle sizes compared to those stabilized by soybean meal hydrolysates (Zhang et al., 2023).

The absolute value of the ζ-potential in an emulsion system correlates directly with its stability. Emulsions with ζ-potential values above 30 mV typically exhibit good electrostatic stability (Y. Zhang et al., 2023). As indicated in Table 4, the ζ-potential of the β-carotene emulsion stabilized by β-Lg-4MBQ-0.4 was higher than that stabilized by β-Lg-4MBQ-0.2, and both exceed the ζ-potential of the emulsion stabilized by native β-Lg. Moreover, there was no significant difference between the ζ-potentials of the β-carotene emulsions stabilized by β-Lg-4MBQ-0.8 and β-Lg-4MBQ-0.4. With increasing concentrations of 4MBQ, the quantity of polyphenols bound to β-Lg rose (Table 1). The deprotonation of introduced phenolic hydroxyl groups in β-Lg neutralizes the positive charges on the protein's side chains (D. Wang et al., 2024). As a result, the ζ-potential of the emulsions stabilized by β-Lg-4MBQ conjugates positively correlates with the 4MBQ concentration. A lower PDI indicates greater uniformity within the emulsion, which consequently enhances its stability (D. Wang et al., 2024). The β-carotene emulsion stabilized by β-Lg-4MBQ-0.4, characterized by the smallest particle size and PDI as well as the highest ζ-potential, demonstrated the greatest stability among emulsions stabilized by all β-Lg-4MBQ conjugates.

Table 4
The particle size, PDI and ζ-potential of β-carotene emulsion stabilized by β-Lg and β-Lg-4MBQ conjugates.

Emulsifier	Particle size(nm)	PDI(%)	ζ-potential(mV)
β-Lg	395.27 ± 3.34^{a}	44.83 ± 1.99^{a}	−37.17 ± 0.25^{c}
β-Lg-4MBQ-0.2	329.87 ± 9.53^{c}	32.73 ± 1.60^{b}	−40.33 ± 0.32^{b}
β-Lg-4MBQ-0.4	308.33 ± 6.79^{d}	24.43 ± 1.98^{c}	−43.77 ± 0.50^{a}
β-Lg-4MBQ-0.8	347.05 ± 6.14^{b}	44.60 ± 1.71^{a}	−43.60 ± 0.36^{a}

Note: Different superscript lowercase letters indicate significant differences between different samples ($P < 0.05$).

3.10.2. β-carotene retention and lipid oxidation in emulsions under thermal, light exposure and storage treatment

The retention rate of β-carotene is a critical indicator for assessing the stability of β-carotene emulsions. This study examined the retention rate of β-carotene stabilized by β-Lg-4MBQ-0.4 under various conditions including heating, light exposure, and storage.

The β-carotene content in emulsions stabilized with both β-Lg and β-Lg-4MBQ-0.4 decreased with increasing thermal treatment temperatures, duration of light exposure and storage periods (Fig. 4a-4c). At 50 °C for 30 min, the retention rate of β-carotene in β-Lg-4MBQ-0.4-stabilized emulsions was 88.39 ± 1.07 %, similar to that in β-Lg-stabilized emulsions ($P > 0.05$). However, at temperatures from 60 °C to 90 °C, β-carotene retention was significantly higher in emulsions stabilized by β-Lg-4MBQ-0.4 compared to those stabilized by β-Lg. This may be partly attributed to the enhanced thermal stability of β-Lg-4MBQ conjugates compared to native β-Lg. Additionally, after 2, 4, 6, and 8 h of light exposure, and during dark storage for 3, 6, 9, 12, and 15 days, the retention rates of β-carotene in β-Lg-4MBQ-0.4-stabilized emulsions consistently exceeded those in β-Lg-stabilized emulsions. This suggests that the β-Lg-4MBQ conjugates formed through the reaction of β-Lg with 4MBQ enhances the thermal, light, and storage stability of β-carotene emulsions compared to those stabilized by β-Lg alone. The components in food emulsions that induce lipid oxidation, such as transition metal ions, and enzymes, are predominantly situated in the aqueous phase. These components or the free radicals they generate diffuse to the oil-water interface, initiating lipid oxidation at this interface and subsequently penetrating into the interior of oil droplets (McClements et al., 2018). β-Lg-4MBQ-0.4, in contrast to native β-Lg, exhibited heightened antioxidant properties, effectively enhancing the antioxidant capacity of the oil-water interface and thereby stabilizing β-carotene within the oil phase. Furthermore, emulsions stabilized by β-Lg-4MBQ-0.4 exhibited smaller particle size and higher ζ-potential compared to those stabilized by β-Lg (Table 4). Therefore, β-Lg-4MBQ-0.4 effectively reduces the likelihood of emulsion flocculation and coalescence, thereby enhancing the stability of β-carotene (D. Wang et al., 2024).

Fresh emulsions stabilized by β-Lg-4MBQ-0.4 and β-Lg showed TBARS values of approximately 4.25 mg/kg and 3.63 mg/kg, respectively, both above 0 mg/kg, indicating oxidation products likely originated from raw materials or during emulsion preparation (Fig. 4d). Following 8 h of light exposure, 30 min heating at 90 °C, or 15 day storage in darkness, emulsions stabilized by β-Lg-4MBQ-0.4 exhibited significantly lower TBARS values compared to those stabilized by β-Lg (Fig. 4d). This is consistent with the results of β-carotene retention, as both are attributed to the higher antioxidant capacity of β-Lg-4MBQ-0.4 compared to β-Lg. This finding is also in line with the results reported by

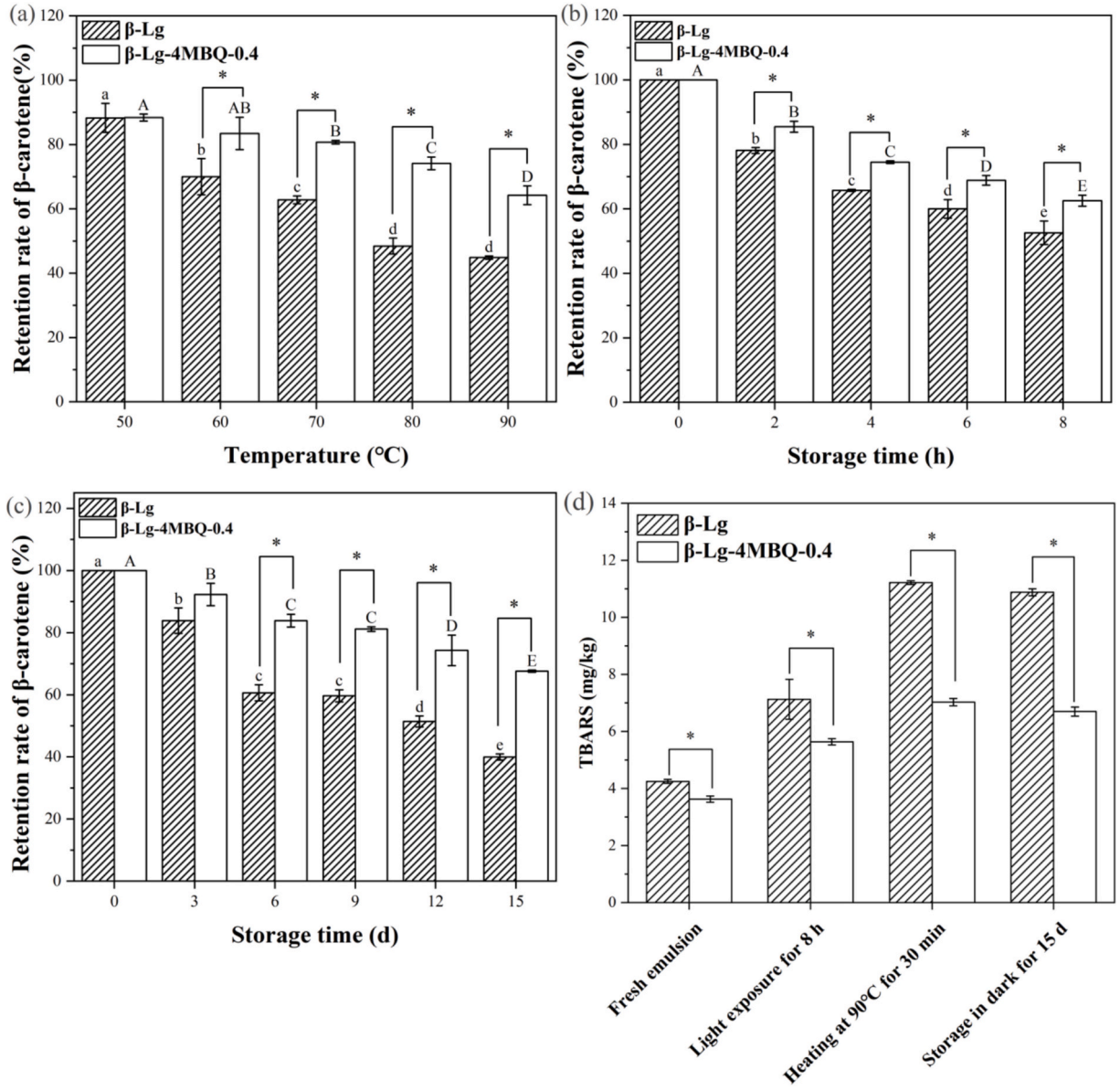

Fig. 4. The retention rate of β-carotene in emulsions stabilized by β-Lg and β-Lg-4MBQ-0.4: heating for 30 mins (a), natural light exposure (b), dark storage (c), and TBARS value of representative β-carotene emulsions (d). Different letters represent significant differences among treatments using the same emulsifier, and * indicates significant differences among emulsifiers under identical treatment conditions ($P < 0.05$).

Huang et al. (2024).

4. Conclusion

A higher content of 4MBQ increased the potential of reactive groups in β-Lg involved in reactions with 4MBQ, leading to elevated total phenolic content and reduced levels of free amino and thiol groups. The reaction between 4MBQ and β-Lg significantly altered the protein's structure. β-Lg-4MBQ conjugates exhibited markedly enhanced thermal stability, H_0, EAI, ESI, and antioxidant properties compared to native β-Lg. Moreover, these properties of β-Lg-4MBQ conjugates improved with increasing 4MBQ content. The β-Lg-4MBQ conjugates exhibited superior emulsifying and antioxidative properties compared to β-Lg, making them effective as antioxidant emulsifiers. Among these, β-Lg-4MBQ-0.4 demonstrated the highest stabilizing effect on β-carotene emulsions. Emulsions stabilized by β-Lg-4MBQ-0.4 showed significantly enhanced stability under heat treatment, light exposure, and storage compared to those stabilized by β-Lg. These findings provide a scientific basis for rational enhancement of protein functional properties through food component interactions, and offer theoretical guidance for developing nutritionally fortified foods incorporating lipid-soluble bioactive compounds. For polyphenols such as chlorogenic acid and rosmarinic acid, whose oxidative products have failed to be synthesized through electrochemical oxidation, determining the quantity of quinone compounds formed during their covalent interaction with proteins, as well as the impact of quinone concentration on the structure and functionality of the resulting conjugates, remains an area that requires further investigation.

CRediT authorship contribution statement

Jinshun Ye: Writing – original draft, Investigation. **Xiaotong Li:** Investigation. **Zhenzhao Weng:** Investigation. **Yuting Li:** Writing – review & editing, Project administration, Methodology, Funding acquisition. **Xiaozhen Liu:** Validation. **Xiangying Yu:** Validation. **Fengyuan Liu:** Methodology. **Jingkun Yan:** Writing – review & editing. **Lin Li:**

Writing – review & editing.

Declaration of competing interest

The authors declare that they have no known competing financial interests or personal relationships that could have appeared to influence the work reported in this paper.

Acknowledgements

This work was supported by the National Natural Science Foundation of China (No. 32272320 & 31701727), the Dongguan Key R&D Programme (2022120030008) and Foundation for Innovation Team in Higher Education of Guangdong, China (2021KCXTD035). The ATR-FTIR and CD spectroscopy data were obtained using equipment maintained by Dongguan University of Technology Analytical and Testing Center.

Data availability

Data will be made available on request.

References

Ali, M., Keppler, J. K., Coenye, T., & Schwarz, K. (2018). Covalent whey protein–rosmarinic acid interactions: A comparison of alkaline and enzymatic modifications on physicochemical, antioxidative, and antibacterial properties. *Journal of Food Science, 83*(8), 2092–2100. https://doi.org/10.1111/1750-3841.14222

Al-Shabib, N. A., Khan, J. M., Malik, A., Alsenaidy, M. A., Rehman, M. T., AlAjmi, M. F., … Khan, R. H. (2018). Molecular insight into binding behavior of polyphenol (rutin) with beta lactoglobulin: Spectroscopic, molecular docking and MD simulation studies. *Journal of Molecular Liquids, 269*, 511–520. https://doi.org/10.1016/j.molliq.2018.07.122

Chen, G., Wang, S., Feng, B., Jiang, B., & Miao, M. (2019). Interaction between soybean protein and tea polyphenols under high pressure. *Food Chemistry, 277*, 632–638. https://doi.org/10.1016/j.foodchem.2018.11.024

Chi, E. Y., Krishnan, S., Randolph, T. W., & Carpenter, J. F. (2003). Physical stability of proteins in aqueous solution: Mechanism and driving forces in nonnative protein aggregation. *Pharmaceutical Research, 20*, 1325–1336. https://doi.org/10.1023/A:1025771421906

Dai, K., Wang, J., Luo, Y., Tu, Y., Ren, F., & Zhang, H. (2023). Characteristics and functional properties of maillard reaction products from α-lactalbumin and polydextrose. *Foods, 12(15), Article 2866*. https://doi.org/10.3390/foods12152866

Dai, T., Li, T., Li, R., Zhou, H., Liu, C., Chen, J., & McClements, D. J. (2020). Utilization of plant-based protein-polyphenol complexes to form and stabilize emulsions: Pea proteins and grape seed proanthocyanidins. *Food Chemistry, 329, Article 127219*. https://doi.org/10.1016/j.foodchem.2020.127219

Dimakou, C., & Oreopoulou, V. (2012). Antioxidant activity of carotenoids against the oxidative destabilization of sunflower oil-in-water emulsions. *LWT-Food Science and Technology, 46*(2), 393–400. https://doi.org/10.1016/j.lwt.2011.12.013

Ding, J., Qiu, X., Li, Y., Wang, Y., Mao, Y., Yang, C., & Sun, Y. (2024). Preparation and characterization of protein-antioxidant complex Pickering particles for high internal phase emulsions. *Food Hydrocolloids, 151, Article 109861*. https://doi.org/10.1016/j.foodhyd.2024.109861

Fan, L., Xie, P., Wang, Y., Liu, X., Li, Y., & Zhou, J. (2019). Influences of mannosylerythritol lipid-a on the self-assembling structure formation and functional properties of heat-induced β-lactoglobulin aggregates. *Food Hydrocolloids, 96*, 310–321. https://doi.org/10.1016/j.foodhyd.2019.05.033

Fei, X., Yan, Y., Wang, L., Huang, Z., Gong, D., & Zhang, G. (2023). Protocatechuic acid and gallic acid improve the emulsion and thermal stability of whey protein by covalent binding. *Food Research International, 170, Article 113000*. https://doi.org/10.1016/j.foodres.2023.113000

Han, X., Liang, Z., Tian, S., Liu, L., & Wang, S. (2022). Epigallocatechin gallate (EGCG) modification of structural and functional properties of whey protein isolate. *Food Research International, 158*. https://doi.org/10.1016/j.foodres.2022.111534. Article 111534.

Huang, X., Xia, B., Liu, Y., & Wang, C. (2024). Non-covalent interactions between rice protein and three polyphenols and potential application in emulsions. *Food Chemistry, X, 22, Article 101459*. https://doi.org/10.1016/j.fochx.2024.101459

Jiang, Z., Li, T., Ma, L., Chen, W., Yu, H., Abdul, Q., Hou, J., & Tian, B. (2020). Comparison of interaction between three similar chalconoids and α-lactalbumin: Impact on structure and functionality of α-lactalbumin. *Food Research International, 131, Article 109006*. https://doi.org/10.1016/j.foodres.2020.109006

Jing, H., Sun, J., Mu, Y., Obadi, M., McClements, D. J., & Xu, B. (2020). Sonochemical effects on the structure and antioxidant activity of egg white protein–tea polyphenol conjugates. *Food & Function, 11*(8), 7084–7094. https://doi.org/10.1039/D0FO01636E

Ke, C., & Li, L. (2024). Modification mechanism of soybean protein isolate-soluble soy polysaccharide complex by EGCG through covalent and non-covalent interaction: Structural, interfacial, and functional properties. *Food Chemistry, 448, Article 139033*. https://doi.org/10.1016/j.foodchem.2024.139033

Lee, M.-R., Choi, H.-N., Ha, H.-K., & Lee, W.-J. (2013). Production and characterization of beta-lactoglobulin/alginate nanoemulsion containing coenzyme Q10: Impact of heat treatment and alginate concentrate. *Korean Journal for Food Science of Animal Resources, 33*(1), 67–74. https://doi.org/10.5851/kosfa.2013.33.1.67

Li, Y., Jongberg, S., Andersen, M. L., Davies, M. J., & Lund, M. N. (2016). Quinone-induced protein modifications: Kinetic preference for reaction of 1, 2-benzoquinones with thiol groups in proteins. *Free Radical Biology and Medicine, 97*, 148–157. https://doi.org/10.1016/j.freeradbiomed.2016.05.019

Li, Y., Li, X., Ye, J., Weng, Z., Liu, X., Liu, F., Yan, J., & Li, L. (2024). Reactivity of amino acid residues towards 4-methylbenzoquinone: Effect on the site-specificity of quinone-protein reaction. *LWT-food. Science and Technology, 200, Article 116217*. https://doi.org/10.1016/j.lwt.2024.116217

Lino, R. C., Carvalho, S. M. D., Noronha, C. M., Sganzerla, W. G., Rosa, C. G. D., Nunes, M. R., & Barreto, P. L. M. (2020). Development and characterization of poly-ε-caprolactone nanocapsules containing β-carotene using the nanoprecipitation method and optimized by response surface methodology. *Brazilian Archives of Biology and Technology, 63, Article e20190184*. https://doi.org/10.1590/1678-4324-2020190184

Liu, G., Hu, M., Du, X., Liao, Y., Yan, S., Zhang, S., Qi, B., & Li, Y. (2022). Correlating structure and emulsification of soybean protein isolate: Synergism between low-pH-shifting treatment and ultrasonication improves emulsifying properties. *Colloids and Surfaces A: Physicochemical and Engineering Aspects, 646, Article 128963*. https://doi.org/10.1016/j.colsurfa.2022.128963

Liu, J., Engholm-Keller, K., Poojary, M. M., Bevilacqua, M., Andersen, M. L., & Lund, M. N. (2024). Reactivity and mechanism of the reactions of 4-methylbenzoquinone with amino acid residues in β-lactoglobulin: A kinetic and product investigation. *Food Chemistry, 434, Article 137473*. https://doi.org/10.1016/j.foodchem.2023.137473

Man, P., Sun, L., Han, X., Zhang, H., Qin, L., & Ren, H. (2024). Effects of different tea polyphenols conjugated with β-lactoglobulin on antioxidant capacity and structural properties. *LWT-food. Science and Technology, 198, Article 115990*. https://doi.org/10.1016/j.lwt.2024.115990

McClements, D. J. (2002). Theoretical prediction of emulsion color. *Advances in Colloid and Interface Science, 97*(1–3), 63–89. https://doi.org/10.1016/S0001-8686(01)00047-1

McClements, D. J., & Decker, E. (2018). Interfacial antioxidants: A review of natural and synthetic emulsifiers and coemulsifiers that can inhibit lipid oxidation. *Journal of Agricultural and Food Chemistry, 66*(1), 20–35. https://doi.org/10.1021/acs.jafc.7b05066

Pham, L. B., Wang, B., Zisu, B., & Adhikari, B. (2019). Complexation between flaxseed protein isolate and phenolic compounds: Effects on interfacial, emulsifying and antioxidant properties of emulsions. *Food Hydrocolloids, 94*, 20–29. https://doi.org/10.1016/j.foodhyd.2019.03.007

Qian, C., Decker, E. A., Xiao, H., & McClements, D. J. (2012). Physical and chemical stability of β-carotene-enriched nanoemulsions: Influence of pH, ionic strength, temperature, and emulsifier type. *Food Chemistry, 132*(3), 1221–1229. https://doi.org/10.1016/j.foodchem.2011.11.091

Simion, A.-M., Aprodu, I., Dumitraşcu, L., Bahrim, G. E., Alexe, P., & Stănciuc, N. (2015). Exploring the heat-induced structural changes of β-lactoglobulin-linoleic acid complex by fluorescence spectroscopy and molecular modeling techniques. *Journal of Food Science and Technology, 52*, 8095–8103. https://doi.org/10.1007/s13197-015-1949-2

Sun, J., Liu, T., Zhang, F., Huang, Y., Zhang, Y., & Xu, B. (2022). Tea polyphenols on emulsifying and antioxidant properties of egg white protein at acidic and neutral pH conditions. *LWT - Food Science and Technology, 153, Article 112537*. https://doi.org/10.1016/j.lwt.2021.112537

Wang, D., Li, H., Hou, T.-Y., Zhang, Z.-J., & Li, H.-Z. (2024). Effects of conjugated interactions between Perilla seed meal proteins and different polyphenols on the structural and functional properties of proteins. *Food Chemistry, 433, Article 137345*. https://doi.org/10.1016/j.foodchem.2023.137345

Wang, Y., Zhang, P., Lin, H., Fei, X., Zhang, G., & Hu, X. (2024). Covalent binding of β-Lactoglobulin and rosmarinic acid by alkaline and free-radical treatment: Improved thermal stability and antioxidant capability. *Food. Bioscience, 61, Article 104574*. https://doi.org/10.1016/j.fbio.2024.104574

Waqar, K., Engholm-Keller, K., Joehnke, M. S., Chatterton, D. E., Poojary, M. M., & Lund, M. N. (2022). Covalent bonding of 4-methylcatechol to β-lactoglobulin results in the release of cysteine-4-methylcatechol adducts after in vitro digestion. *Food Chemistry, 397, Article 133775*. https://doi.org/10.1016/j.foodchem.2022.133775

Wu, T., Lin, L., Zhang, X., Wang, X., & Ding, J. (2023). Covalent modification of soy protein hydrolysates by EGCG: Improves the emulsifying and antioxidant properties. *Food Research International, 164, Article 112317*. https://doi.org/10.1016/j.foodres.2022.112317

Xu, J., Hao, M., Sun, Q., & Tang, L. (2019). Comparative studies of interaction of β-lactoglobulin with three polyphenols. *International Journal of Biological Macromolecules, 136*, 804–812. https://doi.org/10.1016/j.ijbiomac.2019.06.053

Xue, Y.-T., Han, Y.-N., Wang, Y., Zhang, Y.-H., Yin, Y.-Q., Liu, B.-H., & Zhao, X.-H. (2023). Effect of ferulic acid covalent conjugation on the functional properties and antigenicity of β-lactoglobulin. *Food Chemistry, 406, Article 135095*. https://doi.org/10.1016/j.foodchem.2022.135095

Yan, X., Gao, Y., Liu, S., Zhang, G., Zhao, J., Cheng, D., & Gong, D. (2021). Covalent modification by phenolic extract improves the structural properties and antioxidant

activities of the protein isolate from Cinnamomum camphora seed kernel. *Food Chemistry, 352, Article 129377*. https://doi.org/10.1016/j.foodchem.2021.129377

Yin, J., Hedegaard, R., Skibsted, L. H., & Andersen, M. L. (2014). Epicatechin and epigallocatechin gallate inhibit formation of intermediary radicals during heating of lysine and glucose. *Food Chemistry, 146*, 48–55. https://doi.org/10.1016/j.foodchem.2013.09.032

Zhang, L., Lu, Y., Ye, Y.-H., Yang, S.-H., Tu, Z.-C., Chen, J., & Yuan, T. (2018). Insights into the mechanism of quercetin against BSA-fructose glycation by spectroscopy and high-resolution mass spectrometry: Effect on physicochemical properties. *Journal of Agricultural and Food Chemistry, 67*(1), 236–246. https://doi.org/10.1021/acs.jafc.8b06075

Zhang, M., Fan, L., Liu, Y., & Li, J. (2023). Migration of gallic acid from the aqueous phase to the oil–water interface using pea protein to improve the physicochemical stability of water–in–oil emulsions. *Food Hydrocolloids, 135, Article 108179*. https://doi.org/10.1016/j.foodhyd.2022.108179

Zhang, X., Yin, C., Hao, J., Ma, D., Li, Z., Li, Y., & Qi, B. (2023). Improving the biological activity, functional properties, and emulsion stability of soybean meal hydrolysate via covalent conjugation with polyphenol. *Food Chemistry, 422*, Article 136255. https://doi.org/10.1016/j.foodchem.2023.136255

Zhang, Y., Zhang, T., Dong, C., Zhao, R., Zhang, X., & Wang, C. (2023). Lycopene-loaded emulsions stabilized by whey protein covalently modified with pectin or/and chlorogenic acid: Enhanced physicochemical stability and reduced bio-accessibility. *Food Chemistry, 417*, Article 135879. https://doi.org/10.1016/j.foodchem.2023.135879